



Fluoride ion removal from aqueous solution, groundwater, and seawater by granular and powdered *Conocarpus erectus* biochar

Fatemeh Papari^a, Parham Rouhi Najafabadi^a, Bahman Ramavandi^{b,*}

^aDepartment of Chemical Engineering, Bushehr Branch, Islamic Azad University, Bushehr, Iran, emails: fatemeh.papari@yahoo.com (F. Papari), parham.rouhi@gmail.com (P.R. Najafabadi)

^bEnvironmental Health Engineering Department, Faculty of Health, Bushehr University of Medical Sciences, Sabzabad Bolvd., Bahmani, Bushehr 7518759577, Iran, Tel. +989363311903; Fax: +9877334550134; emails: ramavandi_b@yahoo.com, b.ramavandi@bpums.ac.ir

Received 16 May 2016; Accepted 16 October 2016

ABSTRACT

This paper reports on the development of granular and powdered biochar of *Conocarpus erectus* (GBC and PBC) for the removal of fluoride ions from aqueous solution. The surface and adsorption characteristics of the fresh and used samples of GBC and PBC were analyzed by fourier transform infrared spectroscopy (FTIR), Brunauer–Emmett–Teller (BET), and scanning electron microscope (SEM). The parameters affecting the adsorption capacity, such as the pH (2–12), initial fluoride concentration (5–10 mg/L), contact time (3–80 min), adsorbent dosage (2–15 g/L), mixing velocity (0–150 rpm), temperature (20°C–50°C), and co-existing ions, have been evaluated. The results show that the maximum removal of fluoride (PBC: 98.5% and GBC: 80%) was achieved at pH 6 for both adsorbents. The adsorption data obtained at 23°C were fitted to the Langmuir model slightly better than to other isotherms (PBC: 205.7 mg/g and GBC: 13.17 mg/g), and they were also fitted to a pseudo-second-order kinetics model. After seven times of reuse, the adsorption efficiency of PBC and GBC reached 70.1% and 49.6%, respectively. The thermodynamic study indicated that the fluoride adsorption process by both adsorbents is exothermic in nature. In order to assess the practical utility of the studied adsorbents, batch studies were carried out with two real samples (fluoride contaminated groundwater and seawater). The PBC adsorbent is a more effective adsorbent than the GBC for the reduction of fluoride ion levels to the standard permissible limit (1.5 mg/L).

Keywords: *Conocarpus erectus*; Fluoride ion; Biochar; Adsorption; Granular; Powdered

1. Introduction

Fluoride contamination of water resources through a combination of natural processes and human activity is a major concern worldwide [1,2]. According to the literature [3,4], more than 250 million people in China, India, Pakistan, southern America, and Iran regularly drink fluoride contaminated water that exceeds the present WHO guideline of 1.5 mg/L. Excessive intake of fluoride can cause harmful effects on neurotransmitters and fetal cerebral function, or conditions such as skeletal/dental fluorosis [1,4]. Considering

these serious health effects, several technologies, including precipitation, ion exchange, membrane separation, electro dialysis, and adsorption, have been developed for fluoride removal [5]. To effectively remove the excess fluoride in water, adsorption is considered one of the most attractive methods because of the low production cost and simplicity in design and operation [6,7].

Activated carbon, a typical and ideal adsorbent for water and wastewater treatment, is frequently made from non-renewable coal [8], and its production is not cost-effective due to the high energy consumption required for it. Researchers have been exploring new precursors and methods to prepare adsorbents for use in water/wastewater samples. Biochar is an efficient adsorbent in the removal of contaminants from

* Corresponding author.

aqueous solution, has a low energy cost, and can be obtained from renewable and abundant precursors in comparison with activated carbon [9]. Moreover, according to the International Biochar Initiative (IBI) and the literature [8,10–14], the specific properties of biochar, including its large specific surface area, surface porosity, enriched surface functional groups, and inorganic components, make it an ideal adsorbent to remove pollutants from aqueous solution.

Biochar is produced from resources such as wood [15], vegetable waste [16], olives [16], or *Phoenix dactylifera* [17] for the efficient removal of inorganic and organic pollutants from waters and wastewaters. In this regard, Mohan et al. [8] reported that biochar produced from pinewood and pine bark can remove fluoride from water effectively and also that these low surface area chars ($S_{\text{BET}} = 1\text{--}3 \text{ m}^2/\text{g}$) can remove similar or larger amounts of fluoride than activated carbon ($S_{\text{BET}} = 1,000 \text{ m}^2/\text{g}$). Recently, the removal of contaminants from water by biochar was reviewed [18]. Despite these reviews, knowledge on the practical application of biochar for water treatment is limited. Therefore, it is necessary to assess the applicability of biochar in real water treatment such as fluoride removal from contaminated groundwater.

For this purpose, a variety of natural materials have been tested for fluoride adsorption [19–21]. The various materials studied in the past include coconut fiber [20], *Sargassum sp.* [6], pinewood and pine bark chars [19], wheat straw [22], rice straw [23], and corn stover [21]. Therefore, there is a need for developing low-cost, easily available materials that could allow the economic removal of fluoride ions [5].

Regarding the differences in the adsorption capacity of various adsorbents as well as their cost, variety, and ease of access, the use of regional adsorbents has been investigated to evaluate their applicability. The *Conocarpus erectus* tree is a fast-growing and common plant in southern Iran, especially in the surrounding area of Bushehr city, and it is easily prepared and used. This tree is an evergreen plant cultured in many areas of the world such as North, Central, and South America, western Africa, and mildest and mediterranean countries. Furthermore, *C. erectus* trees are pruned twice a year in these countries, and thus, a huge waste is produced annually. A literature survey indicated that adsorption study of fluoride with *C. erectus* branches as the adsorbent has not been carried out to date, and this is the first such study undertaken by the authors.

Thus, the purpose of this study is the use of granular and powdered biochar of *C. erectus* (GBC and PBC) in fluoride removal from water and the evaluation and comparison of their efficiency. Parametric optimization, adsorbent characterization, isotherm and kinetic studies, thermodynamic evaluation, reusability of the adsorbent, and competitive ion impact assessment were also carried out. The adsorption properties of both GBC and PBC branches in field conditions were tested with two real samples (groundwater and seawater).

2. Experimental setup

2.1. Chemicals

All the primary materials used in this study, sodium fluoride (99% purity), sodium hydroxide, and hydrochloric acid,

were supplied by Merck Co., India. The materials were of analytical grade and applied without further purification. A working solution was prepared by mixing a sodium fluoride stock solution with doubly distilled water. The fluoride stock solution was prepared by dissolving 2.2101 g of sodium fluoride (NaF) in 1,000 mL of doubly distilled water.

2.2. Production of biochar from *C. erectus*

Dried *C. erectus* wood was used as the base material for the preparation of biochar. The *C. erectus* wood was locally collected as discarded pruning waste and was first debarked and then crushed into small pieces (2–4 cm). The wood particles were washed, dried (at 105°C during 24 h), and then pyrolyzed at 350°C for 2 h in the absence of oxygen. After that, the pyrolyzed pieces were ground and finally passed through 40 and 120 mesh sieves to obtain biochar powder ($\Phi = 0.125\text{--}0.4 \text{ mm}$) and 10 and 14 mesh sieves to obtain biochar granules ($\Phi = 1.14\text{--}2 \text{ mm}$) for use in the adsorption tests.

2.3. Experimental design and procedure

Batch adsorption studies were carried out in 250 mL Erlenmeyer flasks inside a shaker-incubator. For each of the tests, samples (100 mL) with known concentrations of fluoride were added to the Erlenmeyer flasks. The pH of the solutions was regulated using 0.1 N HCl and NaOH; a certain amount of biochar (PBC or GBC) was added to the flasks; and the suspensions were mixed at 120 rpm. After a certain contact time, the suspensions were filtered using Whatman filter paper No. 42, and the filtrates were analyzed for residual fluoride ions. The main parameters considered were: solution pH (2, 4, 6, 8, 10, and 12), initial fluoride concentration (5, 10, and 15 mg/L), adsorbent dose (2, 5, 8, 10, and 15 g/L), solution temperature (20°C, 25°C, 30°C, 35°C, 40°C, and 50°C), mixing intensity (0, 50, 90, 120, and 150 rpm), and contact time (3, 5, 10, 20, 40, 60, and 80 min for the kinetics tests and 6 h for the equilibrium tests). All the tests were performed twice to ensure the reproducibility of the results, and the average of these two measurements was calculated. A blank test (without PBC or GBC) was carried out for interference control. The adsorption efficiency (AE) and the amount of fluoride adsorbed on the adsorbent, q_e (mg/g), were obtained as follows:

$$AE = \frac{C_0 - C_t}{C_0} \times 100 \quad (1)$$

$$q_e = \frac{V(C_0 - C_e)}{M} \quad (2)$$

where C_0 (mg/L), C_t (mg/L), and C_e (mg/L) are the initial, final, and equilibrium concentrations of fluoride ions, respectively. M (g) is the mass of the adsorbent, and V (L) is the volume of the aqueous phase.

The kinetics of fluoride adsorption with the biochar prepared from *C. erectus* was evaluated using adsorption experiments performed in Erlenmeyer flasks containing 100 mL of 5, 10, and 15 mg/L fluoride solutions at pH 6 into which 1 g of biochar *C. erectus* was added and shaken in a

Table 1
Isotherm and kinetic models and thermodynamic equations used in this study [24,25]

Models	Name	Equation	Plot
Isotherm	Langmuir	$q_e = \frac{Q_m k_L C_e}{1 + k_L C_e}$	$\frac{1}{q_e}$ vs. $\frac{1}{C_e}$
	Freundlich	$q_e = k_F C_e^{1/n}$	$\log q_e$ vs. $\log C_e$
	D-R	$\ln q_e = \ln q_m - K_{DR} \varepsilon^2$	$\ln q_e$ vs. ε^2
Kinetic	Pseudo first order	$q_t = q_e [1 - \exp(-k_1 t)]$	$\log(q_e - q_t)$ vs. t
	Pseudo second order	$q_t = \frac{k_2 q_e^2 t}{1 + k_2 q_e t}$	$\frac{t}{q_t}$ vs. t
Thermodynamic	Gibbs free energy	$\Delta G^\circ = -RT \ln K_{Th}$; $\ln K_{Th} = (\Delta S^\circ/R) - (\Delta H^\circ/RT)$; $\Delta G^\circ = \Delta H^\circ - T\Delta S^\circ$	$\ln K_{Th}$ vs. $1/T$

Note: Q_m – maximum adsorption capacity (mg/g), k_L – Langmuir constant (L/mg), k_F – Freundlich constant (mg/g(L/mg)^{1/n}), K_{DR} – D-R constant (mol²/kJ²), ε – Polanyi potential (J/mol), k_1 – rate constant of pseudo-first-order model (1/min), k_2 – rate constant of pseudo-second-order model (mg/g min), q_t – adsorbed amount at any time (mg/g), q_e – adsorbed amount at equilibrium (mg/g), ΔG° – Gibbs free energy change (kJ/mol), ΔH° – enthalpy change (kJ/mol), ΔS° – entropy change (kJ/mol K), and K_{Th} – thermodynamic equilibrium constant (mL/g).

shaker-incubator (Parsazma model, Iran). The same test was conducted at various times between 3 and 80 min. At the end of each test, the suspension was analyzed. The kinetics of fluoride adsorption on the biochar was modeled using two kinetics models (pseudo first order and pseudo second order) by fitting the results from the tests (Table 1).

Tests to evaluate the adsorption equilibrium were carried out by adding 1 g of PBC and GBC into a series of Erlenmeyer flasks containing 100 mL of various fluoride concentrations (3–20 mg/L) at a fixed pH solution of 6. The mixtures were then stirred for 6 h at 120 rpm and a constant temperature (23°C) to reach equilibrium, after which the fluoride concentration of the suspensions was analyzed. The equilibrium adsorption of fluoride on PBC and GBC was modeled using the Langmuir, Freundlich, and Dubinin–Radushkevich (D-R) isotherm models by fitting the results from the tests (Table 1).

In the present study, the adsorption isotherms and kinetics parameters were calculated by a nonlinear method using the solver add-in in a Microsoft Excel spreadsheet.

The thermodynamics of fluoride adsorption onto PBC and GBC was evaluated using adsorption experiments performed in an Erlenmeyer flask, containing 100 mL of a 10 mg/L solution with pH 6 into which 1 g of adsorbent was added and shaken in a temperature-controlled shaker-incubator. This test was conducted at various temperatures between 20°C and 50°C. At the end of each test, the suspension was analyzed. The thermodynamics of fluoride adsorption onto PBC and GBC was analyzed using the estimated change in adsorption free energy (ΔG°), adsorption enthalpy (ΔH°), and adsorption entropy (ΔS°), as presented in Table 1.

The PBC and GBC samples were regenerated for seven consecutive cycles using a sodium hydroxide (1 mol/L NaOH) solution. The regenerated PBC and GBC samples were then subjected to the fluoride adsorption test under identical experimental conditions: pH 6, initial fluoride concentration of 10 mg/L, contact time of 60 min, mixing velocity at 120 rpm, and solution temperature of 23°C.

2.4. Measurements

The surface analysis including the Brunauer–Emmett–Teller (BET) specific surface area and pore volume of both adsorbents (powder and granular) was carried out by the N₂ adsorption/desorption method at –196°C using a Micromeritics model TriStar II-3020 instrument. The biochar samples were degassed for 24 h at 250°C to remove any adsorbed contaminants or moisture that might have been present on the surface. The manufacturer’s software provided the BET surface area of GBC and PBC using the BET equation within $P/P_0 = 0 - 1$:

$$\frac{1}{v[(P_0/P) - 1]} = \frac{C - 1}{v_m C} \left(\frac{P}{P_0} \right) + \frac{1}{v_m C} \quad (3)$$

where P_0 and P are the saturation and equilibrium pressure of adsorbates at the temperature of adsorption; C is the BET constant; v is the amount of gas adsorbed; and v_m is the amount of monolayer adsorbed gas.

Micrographs of PBC and GBC before and after adsorption were obtained by scanning electron microscopy (SEM; Sirion from FEI). The functional groups involved in the adsorption processes, before and after adsorption, were determined using a Fourier transform infrared (FTIR) spectrometer (NICOLET 5700-FTIR) in the range of 400–4,000 cm⁻¹. The fluoride concentration of all the prepared solutions and filtrates was analyzed by an expandable ion analysis (Orion EA 940 ion meter) according to the method presented in the Standard Methods for the Examination of Water and Wastewater [26]. The solution temperature was determined using a mercury thermometer. The pH at zero-point charge (pH_{zpc}) measurement was performed according to our previous study [27,28]. For this purpose, 50 mL of a 0.01 M NaCl solution as the inert electrolyte was poured into a 100-mL Erlenmeyer flask. Then, the pH was regulated to successive initial values of 2, 4, 6, 8, 10, and 12 using either HCl or NaOH, and a given amount

of biochar (at a 1:200 biochar to liquid ratio) was added to the solution. After a mixing time of 24 h, the final pH was analyzed and plotted vs. the initial pH. The pH at which the curve crossed the line $\text{pH}_{(\text{final})} = \text{pH}_{(\text{initial})}$ was selected as the pH_{zpc} of the respective PBC and GBC. The pH of the working solutions was measured using a pH meter (Sense Ion 378, Hack).

3. Results and discussion

3.1. Characteristics of the adsorbents

The main characteristics of PBC and GBC are presented in Table 2. The pH_{zpc} of both PBC and GBC was found to be similar (around 7.5), showing a positive surface charge in a solution at $\text{pH} < 7.5$ and a negative surface charge in a solution at $\text{pH} > 7.5$. As seen in Table 2, the total pore volume of fresh PBC was around 10% higher than that obtained for GBC. Moreover, the pore volume of PBC after fluoride loading decreased more than that of GBC, indicating a larger occupation of the PBC pore volume by the adsorbate. The average pore size of PBC and GBC was 1.873 and 29.13 nm, confirming that the adsorbents are microporous- and mesoporous-type adsorbents, respectively. The specific BET surface area of PBC and GBC was 9.88 and 5.16 m^2/g , respectively, indicating that the specific surface area of PBC is 1.9 times greater than that of GBC. The smaller particle size of the PBC adsorbent provides a larger surface area for the target pollutant per unit weight of adsorbent. These findings are supported by the results reported in the literature [25,29,30]. These data therefore reveal that the powdered sample possesses a larger specific surface area. The values of the BET C constant for PBC and GBC are 109.34 and 84.20, respectively, which demonstrates that the surface of PBC has a greater chance of interacting with fluoride ions.

The SEM images of PBC and GBC are depicted in Figs. 1(a–d). It is clear from the SEM images that the surface of both adsorbents contains deep and different size cavities. However, the cavities on the surface of the used PBC (Fig. 1(d)) seem to be blocked, which can be attributed to the deposition of fluoride ions over the pores of the PBC surface. A similar morphology has been reported for an adsorbent prepared from *Tecomella undulata* [31] and for activated cotton nut shell carbon [32] for targeted pollutant removal.

3.2. Effect of the parameters

3.2.1. Effect of the pH on adsorption

The adsorption capacity of pollutants from aqueous solution is highly dependent on the pH of the solution [33,34]. Fig. 2 shows the effect of the solution pH on fluoride adsorption by both PBC and GBC adsorbents. As seen in Fig. 2, a similar trend is observed for fluoride adsorption by both adsorbents. However, the AE for PBC is significantly higher than that obtained with GBC. The maximum fluoride adsorption was obtained at a solution pH of 6. This phenomenon can be explained by the pH_{zpc} value. The pH_{zpc} for PBC and GBC was found to be 7.5 and 7.6, respectively. This means that the adsorbent surface is negatively charged at solution pH values above these values, and therefore, fluoride ions are repulsed from the surface, which results in a reduction in fluoride adsorption. At pH values below pH_{zpc} , the surface of PBC and GBC is positively charged, leading to better fluoride ion adsorption through electrostatic attraction. However, under strongly acidic conditions at pH 2–4, fluoride adsorption is reduced due to the formation of weak hydrofluoric acid [29]. Similar results have been reported in the literature [29,34,35].

Fig. 2 also shows the final pH solution. Accordingly, the final pH of the solution originally at pH 6 (at which maximum removal was achieved) increased to around neutral pH. This point can be advantageous for full-scale application from an economical point of view, as there is no need to control the effluent pH before entering the environment. This will result in lower costs for fluoride treatments.

3.2.2. Effect of adsorbents dose

Fig. 3 shows the effect of the PBC and GBC adsorbents dose on fluoride adsorption. As shown in Fig. 3, the removal efficiency of fluoride increased from 23.52% to 99.3% and 15.86% to 82.24% for PBC and GBC, respectively, after increasing the adsorbent loading from 2 to 15 g/L. These results may be attributed to a surface area increment of the adsorbents and also the availability of more adsorption sites resulting from the increase in dosage [36]. Having a closer looking at Fig. 3, it is noticeable that, at dosages higher than 10 g/L, no significant changes in the removal efficiency are observed. This phenomenon may be due to the overlapping of active sites at high dosages, thus resulting in a reduced

Table 2
Main characteristics of PBC and GBC adsorbent used in this study

Parameter (unit)	PBC		GBC	
	Fresh	Used	Fresh	Used
Total pore volume ($P/P_0 = 0.980$) (cm^3/g)	0.376	0.218	0.342	0.297
Mean pore diameter (nm)	1.873	1.201	29.13	21.419
Pores structure	Micropore	Micropore	Mesopore	Mesopore
BET (m^2/g)	9.88	7.31	5.16	4.07
C constant of BET	109.34	86.67	84.20	59.43
pH_{zpc}	7.5	–	7.6	–
Particle size (mm)	0.125–0.4	–	1.14–2	–

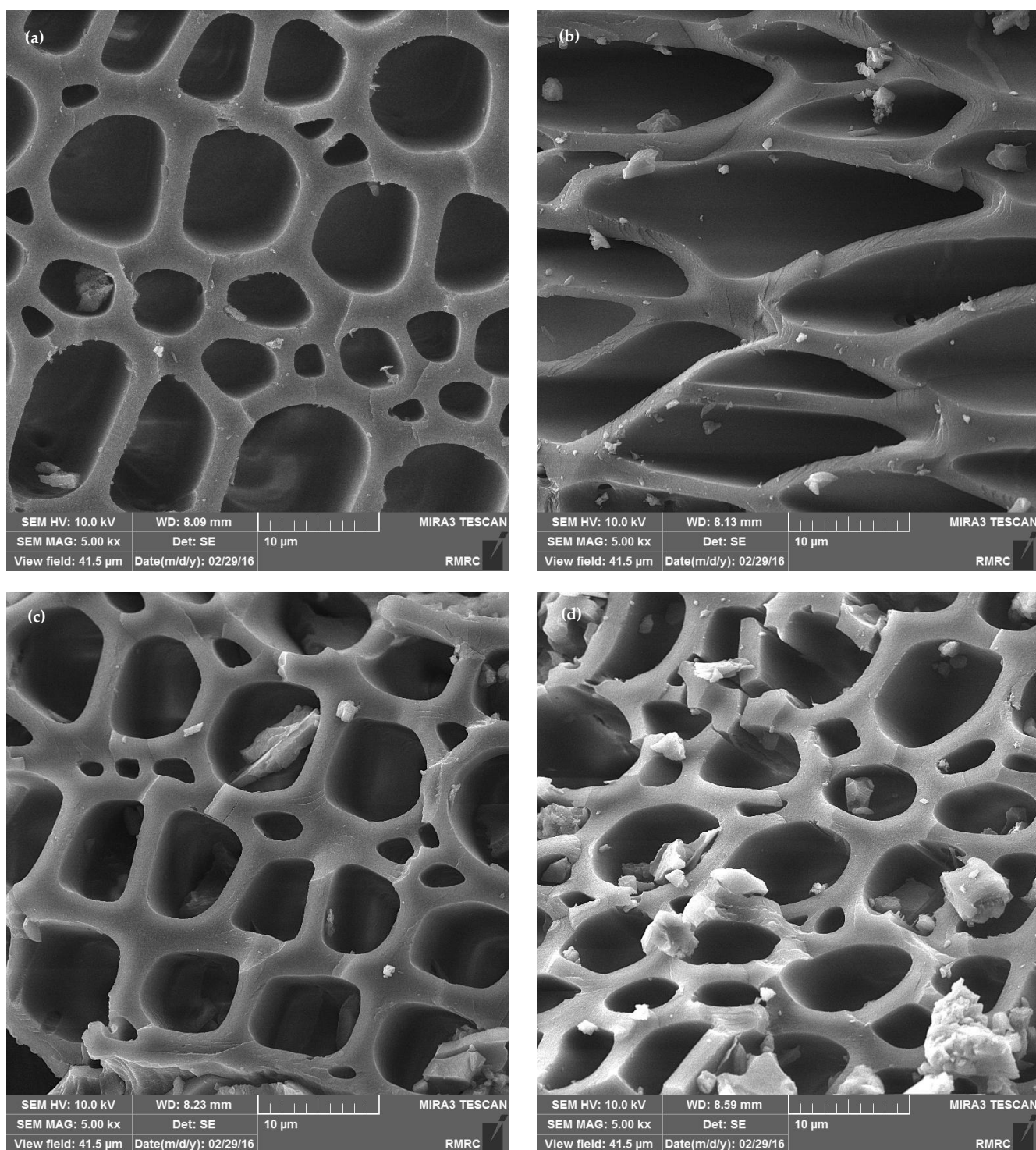


Fig. 1. SEM image of: (a) fresh GBC, (b) used GBC, (c) fresh PBC, and (d) used PBC.

effective surface area for adsorption [25,37]. Therefore, the dose of 10 g/L was selected as the optimum dosage of adsorbent for the rest of the tests. From Fig. 3, the removal efficiency of PBC is higher than that obtained with GBC. The reason could be ascribed to various characteristics, such as the BET surface area and the type and density of functional groups in the adsorbents. For instance, based on Table 2 and

at an adsorbent dose of 10 g/L, the PBC adsorbent provides a surface area of 9.88 m²/g, more than twofold larger than that of GBC (i.e., 4.07 m²/g).

In general, our results are in accordance with those reported in other studies (e.g., [19,29,38]), where an increase in fluoride adsorption was observed with an increase in the adsorbent loading.

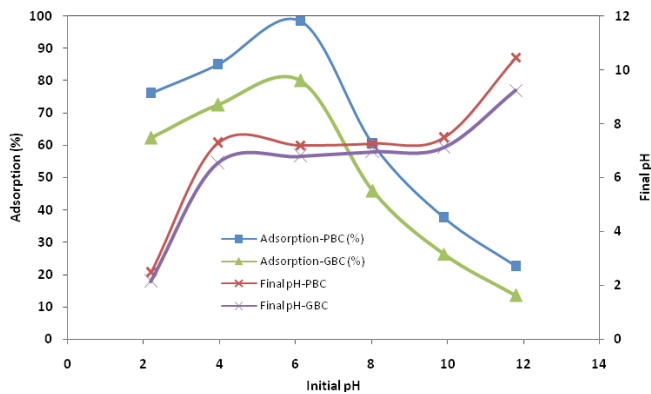


Fig. 2. Effect of solution pH on the fluoride adsorption (adsorbent dose: 10 g/L, fluoride concentration: 10 mg/L, mixing intensity: 120 rpm, contact time: 60 min).

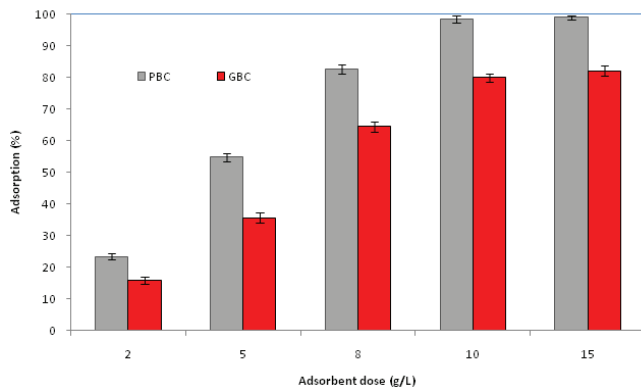


Fig. 3. Effect of adsorbent dose on fluoride adsorption (solution pH: 6, fluoride concentration: 10 mg/L, mixing intensity: 120 rpm, contact time: 60 min).

3.2.3. Effect of contact time and initial fluoride concentration

Figs. 4(a) and (b) demonstrate the influence of various initial concentrations of fluoride (5, 10, and 15 mg/L) on the adsorption as a function of the contact time. It is clear from Figs. 4(a) and (b) that the amount of fluoride adsorbed on both adsorbents increases with the increasing contact time. As shown in Figs. 4 (a) and (b), the percentage of fluoride removal by PBC after 3 min at initial concentrations of 5, 10, and 15 mg/L were measured as 62.05%, 53.36%, and 44.69%, respectively, and the same for GBC were obtained as 44.05%, 34.66%, 26.69%, respectively. By increasing the contact time, the adsorption percentage remarkably increased at each concentration. For instance, after 80 min, fluoride removal percentages of 100%, 99.65%, and 94.09% for PBC and 82.44%, 80.95%, and 76.02% for GBC were obtained at fluoride initial concentrations of 5, 10, and 15 mg/L, respectively. It is obvious from these results that the amount of fluoride adsorbed on both adsorbents increased with the increasing contact time, a result of the fluoride ions in solution having enough time to find free sites on the adsorbent [39]. Furthermore, as seen in Figs. 4(a) and (b) after further increasing the initial fluoride concentration, the percentage of fluoride adsorbed on the adsorbents decreased due to the restriction of free sites

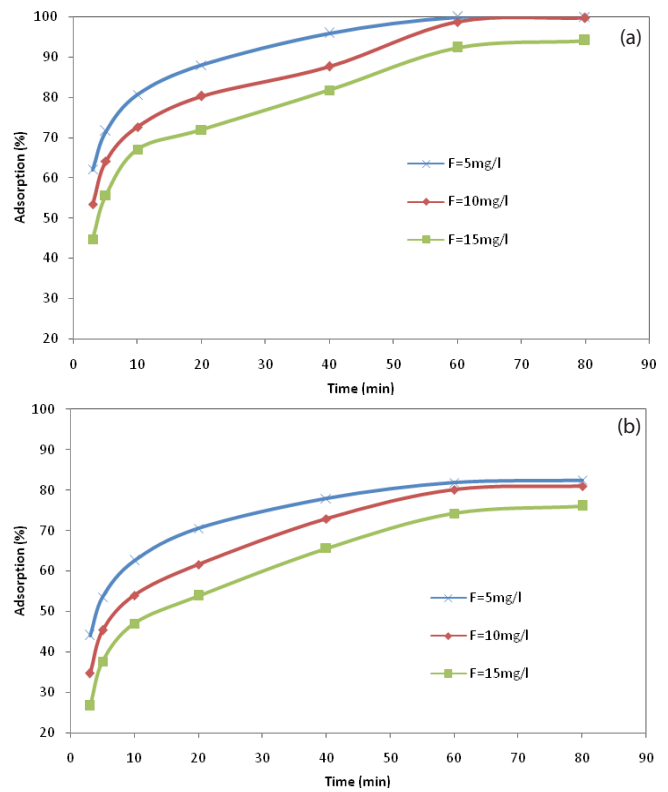


Fig. 4. Effect of contact time and initial fluoride concentration on its removal by: (a) PBC and (b) GBC (adsorbent dose: 10 g/L, solution pH: 6, mixing intensity: 120 rpm).

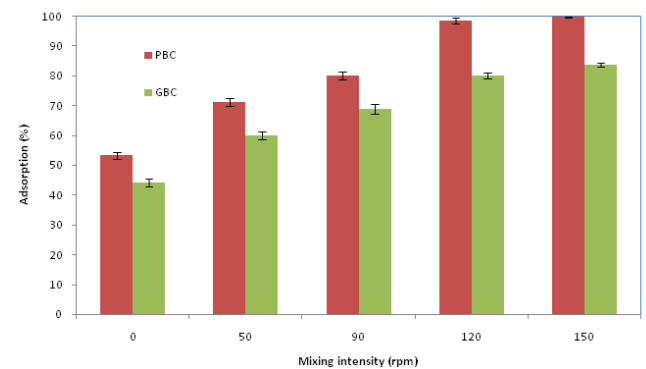


Fig. 5. Effect of mixing intensity on fluoride adsorption (adsorbent dose: 10 g/L, solution pH: 6, fluoride concentration: 10 mg/L, contact time: 60 min).

available for adsorption in the bulk solution at a constant adsorbent content and to a reduction in intraparticle diffusion [23,34]. Thus, F^- adsorption on GBC and PBC depends on the initial fluoride concentration and contact time. Our findings are in agreement with those reported by other researchers [31,40].

3.2.4. Effect of mixing speed

The influence of the mixing velocity (0–150 rpm) on fluoride adsorption is described in Fig. 5. The percentage

of fluoride adsorbed on PBC and GBC without mixing was 53.25% and 44.2%, respectively, and after increasing the mixing velocity to 150 rpm, the percentage of fluoride removal by PBC and GBC increased to 99.7% and 83.7%, respectively. In general, the percentage of adsorbed fluoride increased with the mixing speed for both PBC and GBC. However, according to Fig. 5, increasing the mixing speed was more efficient for fluoride removal by PBC than by GBC. This may be due to an improvement in the diffusion of fluoride ions toward the surface of the adsorbent and a better efficient contact between adsorbate and adsorbent. It is also obvious from Fig. 5 that the percentage of fluoride adsorbed on both adsorbents at a mixing rate beyond 120 rpm did not change. As such, the rate of 120 rpm was selected as the optimal mixing velocity for the next experiments. Scarce reports can be found in the literature regarding the effect of mixing speed on fluoride adsorption by simple adsorbents. However, Khosravi et al. [39], Ismail and AbdelKareem [41], and Rezaee et al. [42] reported that contaminant adsorption increased at elevated mixing speeds.

3.2.5. Effect of solution temperature

Fig. 6 illustrates the influence of the solution temperature on the adsorption of fluoride by PBC and GBC. As observed from Fig. 6, the percentage of fluoride adsorption on PBC and GBC decreased from 98.66% to 85.8% and 80.06% to 65.4%, respectively, as the solution temperature increased from 293 to 323 K. A rise in temperature makes the molecules move away from the interface, thus reducing the adsorption. Sujana et al. [43] presented a plausible reason for the increased desorption by an increase in the thermal energy of the adsorbates. A review of the literature showed that our findings are in accordance with some studies [44] and in conflict with some other [35,45]. The controversy in the literature may be due to differences in the testing conditions and the nature of the adsorbents.

3.2.6. Effect of co-existing ions

Wastewater or groundwater includes many ions that interfere in fluoride adsorption. Hence, it is necessary to estimate their influence on the adsorption process. The most abundant inorganic competing anions present in the natural water are sulfate, nitrate, chloride, and bicarbonate ions [40]. The effect of competitive ions was evaluated at 10 mg/L fluoride concentration by both adsorbents, and the results are shown in Fig. 7. The influence of the sulfate anion on fluoride adsorption was little, but the interference of the nitrate, chloride, and bicarbonate anions was obvious. As for the impact of the later three anions, the decrease in the adsorption rate may be attributed to an increase in the pH value as a result of the hydrolysis of these anions [40]. The same behavior of co-existing anions has also been reported in the literature [23,40,46].

3.3. Modeling study

3.3.1. Adsorption isotherms

Isotherm information can be used to reveal the correlation between the concentration of adsorbate and the applied

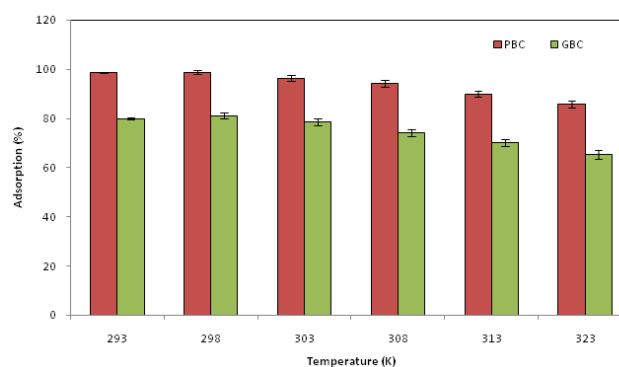


Fig. 6. Effect of solution temperature (adsorbent dose: 10 g/L, solution pH: 6, fluoride concentration: 10 mg/L, mixing intensity: 120 rpm, contact time: 60 min).

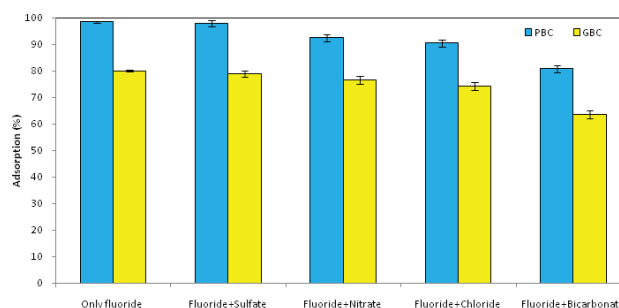


Fig. 7. Effect of co-existing ions (adsorbent dose: 10 g/L, solution pH: 6, fluoride concentration: 10 mg/L, mixing intensity: 120 rpm, contact time: 60 min).

adsorbent, and thus is vital for predicting the maximum adsorption capacity of the adsorbent, an important parameter when designing an adsorption system [47]. The equilibrium adsorption data were analyzed according to the well-known Freundlich, Langmuir, and D–R adsorption isotherms, and used to describe the equilibrium between the adsorbed F⁻ on PBC and GBC and the free fluoride ions in solution at a constant temperature (23°C). Fig. 8 schematically presents the applicability of the isotherm models in the prediction of q_{exp} values using the nonlinear regression method. From Fig. 8, it is clear that the applicability of the isotherm models for the prediction of q_{exp} values is in the order: Langmuir \geq Freundlich \geq D–R. The estimated parameters for the studied isotherms are depicted in Table 3. This table also confirms that the experimental data is better described by the Langmuir model than with the Freundlich and D–R models. This finding demonstrates that monolayer adsorption, rather than Freundlich heterogeneous surface adsorption, plays a key role in the adsorption process.

Using the Langmuir isotherm model (Table 3), the estimated maximum adsorption capacity (Q_m) of GBC and PBC was 13.17 and 205.7 mg/g, respectively, which indicated that the adsorption capacity of PBC is much greater than that of GBC. In recent years, many other adsorbents have been tested for the removal of fluoride from aqueous solution [31,44,48], with adsorption capacities ranging from 6.16 to 118.7 mg/g. The PBC sample studied in this paper is highly competitive

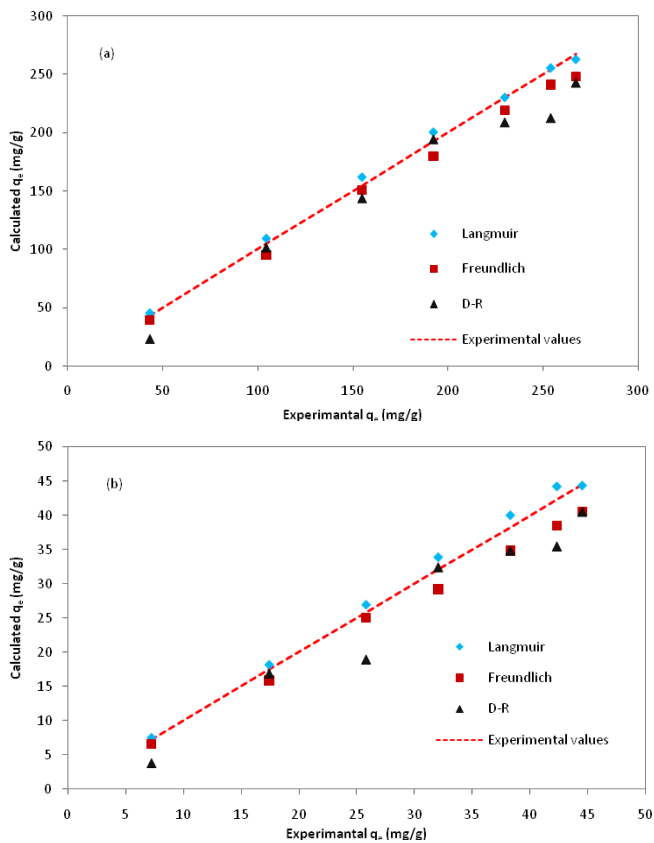


Fig. 8. The calculated q_e values for the isotherm models by using nonlinear regression method vs. experimental q_e values for adsorption of fluoride ions onto: (a) PBC and (b) GBC.

Table 3
Results of isotherm modeling for adsorption of fluoride onto PBC and GBC

Isotherm	Parameter	PBC	GBC
Freundlich	k_f (mg/g)	1.097	1.035
	n	1.133	1.041
	R^2	0.901	0.892
Langmuir	Q_m (mg/g)	205.7	13.17
	K_L (L/mg)	0.005	0.845
	R^2	0.998	0.961
D-R	q_m (mg/g)	12.774	9.235
	K_{DR} (mol ² /kJ ²)	2.00E-09	3.00E-09
	E (kJ/mol)	15.81	12.91
	R^2	0.879	0.869

when compared with most of the adsorbents examined for fluoride adsorption in the recent literature. Furthermore, the main source of PBC is easily available, making the cost of consumables and the manufacture price similar to those of other waste-based adsorbents.

Also, as shown in Table 3, the values of the heterogeneity factor ($1/n$) are less than 1.0, which proves that both PBC and

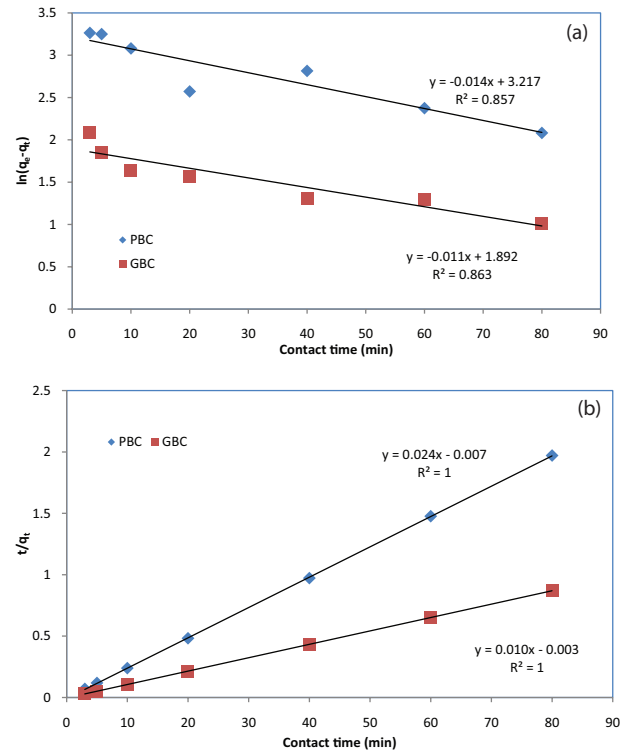


Fig. 9. Kinetic models of: (a) pseudo-first-order model and (b) pseudo-second-order model (adsorbent dose: 10 g/L, solution pH: 6, fluoride concentration: 10 mg/L, mixing intensity: 120 rpm).

GBC are appropriate and beneficial materials for fluoride adsorption [34,49].

Table 3 shows that the experimental data presents also good correlation with the D-R isotherm for both the adsorbents. Regarding the data for the D-R model (Table 3), the amount of free energy of fluoride adsorption for PBC and GBC is 15.81 and 12.91 kJ/mol, respectively. The value of E reveals the mechanism by which adsorption takes place. A value of $E < 8$ kJ/mol indicates physisorption, and a value between 8 and 16 kJ/mol indicates chemisorption [25,47]. Thus, the adsorption of fluoride by PBC and GBC occurs by a mechanism of chemisorption.

3.3.2. Adsorption kinetics

Kinetic studies are required for modeling and designing novel adsorption materials and processes [50]. The fitness of the experimental data to most common kinetic models, pseudo first order and pseudo second order, was evaluated. The kinetic information obtained from the models (depicted in Fig. 9) is presented in Table 4. The fitted linear regression plots show that the experimental data obtained from fluoride adsorption by PBC and GBC are best fitted to the pseudo-second-order model at the investigated concentration (10 mg/L), with higher determination coefficients ($R^2 = 1$) than those for the pseudo-first-order model. Therefore, it was found that the rate of fluoride adsorption onto PBC and GBC is of pseudo second order, suggesting that the adsorption of fluoride on the adsorbents is influenced by both the adsorbate

and the adsorbent concentration under the investigated conditions [19]. In addition, as can be seen from Table 4, the experimental adsorption capacity ($q_{e,exp}$) values were very close to the model-calculated adsorption capacity ($q_{e,cal}$) data, confirming the high correlation of our adsorption results to the pseudo-second-order model. As shown in Table 4, the value of the pseudo-second-order rate constant (k_2) for PCB was more than two times greater than that obtained for GBC under similar experimental conditions. This finding confirms that the rate of mass transfer for PBC is higher than for GBC. A review of the recent literature [5,7,21,51] on the adsorption of fluoride revealed that most researchers have also reported pseudo-second-order model best fits.

3.3.3. Adsorption thermodynamics

The thermodynamic parameters are summarized in Table 5. The values of ΔG° for PBC and GBC were positive at various temperatures, indicating that the nature of adsorption on the adsorbents is not spontaneous under standard conditions. The values of ΔH° were also negative indicating the exothermic nature of the process. Physical and chemical adsorptions are classified by the magnitude of the ΔH° value. When ΔH° falls between 30 and 70 kJ/mol, the adsorption is considered to be chemical adsorption, i.e., a chemical bond is formed between the adsorbate and the adsorbent surface [52]. When ΔH° falls within the range of 0–10 kJ/mol, the adsorption mechanism is considered to be physical adsorption, i.e., the interaction between adsorbent and adsorbate is due to van der Waals forces [52]. Accordingly, chemical

adsorption seems to be the mechanism of fluoride adsorption for PBC and GBC; thus confirming the isotherm results. As seen from Table 5, the negative values of the ΔS° parameter for both adsorbents suggest a decreased randomness at the solid–water interface during the fluoride adsorption process. Analogous thermodynamic parameters have also been reported for the fluoride adsorption with other adsorbents in water or aqueous media [31,53,54].

3.4. Reusability

The main environmental and economical characteristic of an adsorbent is its reusability potential. Therefore, to determine the reusability of PBC and GBC for fluoride adsorption, an experimental phase was carried out. To do this, the reusability of the adsorbents was tested in seven consecutive cycles under identical conditions, where the adsorbents were reused from the previous test without further modification. The fluoride removal efficiency was determined after each test, and the results are depicted in Fig. 10. PBC preserved its adsorption capability after seven uses, whereas the GBC adsorbent was not reusable. Hence, PBC is a stable adsorbent for treating fluoride-laden waters. Overall, the reusable properties of PBC support its potential for commercial use.

3.5. Adsorption mechanism

The results of the FTIR spectrum analysis of the fresh and used PBC and GBC samples are displayed in Fig. 11. The FTIR spectra were similar for PBC and GBC, which confirms that both have identical functional groups. The identified signals for the adsorbents are: 3,062 cm^{-1} ($\equiv\text{C-H}$ and -OH), 1,626 cm^{-1} (-CH=CHR), 1,322 cm^{-1} (-S=O , C-F), 783 cm^{-1} (S-OR esters, -C-H), and 517 cm^{-1} (S-S). The FTIR analysis (Fig. 10) rises several important points. First, sulfur groups in the PBC and GBC structure are observed. Second, there is a vast variety of functional groups on the surface of PBC and GBC (except nitrogen-derived groups). Moreover, by comparing the fresh and used PBC and GBC samples (Fig. 11), the role of certain functional groups in the F^- adsorption by both adsorbents can be discerned, as revealed by the changes in the FTIR peaks of the fresh and used samples. Mariappan et al. [32] reported that the changes in the intensity of the transmittance in FTIR signals for an adsorbent before and after adsorption suggest a chemisorption mechanism in the adsorption process.

Table 4
Kinetic parameter from fitting of experimental data onto kinetic models

Kinetic model	Parameters	PBC value	GBC value
Pseudo first order	k_1 (1/min)	0.014	0.011
	$q_{e,cal}$ (mg/g)	24.95	6.63
	$q_{e,exp}$ (mg/g)	43.53	98.68
	R^2	0.857	0.863
Pseudo second order	k_2 (g/mg/min)	0.082	0.033
	$q_{e,cal}$ (mg/g)	41.66	100
	$q_{e,exp}$ (mg/g)	43.53	98.68
	R^2	1	1

Table 5
Thermodynamic parameters for the adsorption of fluoride ions onto PBC and GBC

Equation	Parameter	Adsorbent	Solution temperature (K)					
			293	298	303	308	313	323
GBC: $y = -29.872x - 8,688.6$	ΔG° (kJ/mol)	GBC	2,516.3	2,559.75	2,603.2	2,646.65	2,690.1	2,777
PBC: $y = -30.6x - 8,646$		PBC	2,500.92	2,544.12	2,587.32	2,630.52	2,673.72	2,760.12
	ΔH° (kJ/mol)	GBC	-29.87					
		PBC	-30.60					
	ΔS° (kJ/mol)	GBC	-8.69					
		PBC	-8.64					

3.6. Treatment of real F⁻ laden water samples by PBC and GBC

Water samples collected from a well (groundwater sample) near Dashtestan, Iran, and the Persian Gulf (as a sophisticated medium) were taken for analysis; their specifications are presented in Table 6. The real samples were treated using

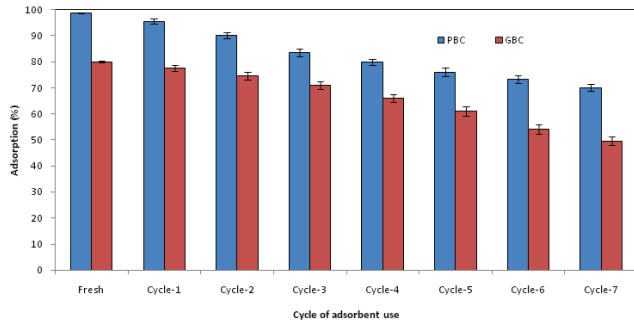


Fig. 10. Effects of adsorbent reuse times on fluoride adsorption (adsorbent dose: 10 g/L, solution pH: 6, fluoride concentration: 10 mg/L, contact time: 60 min; mixing intensity: 120 rpm).

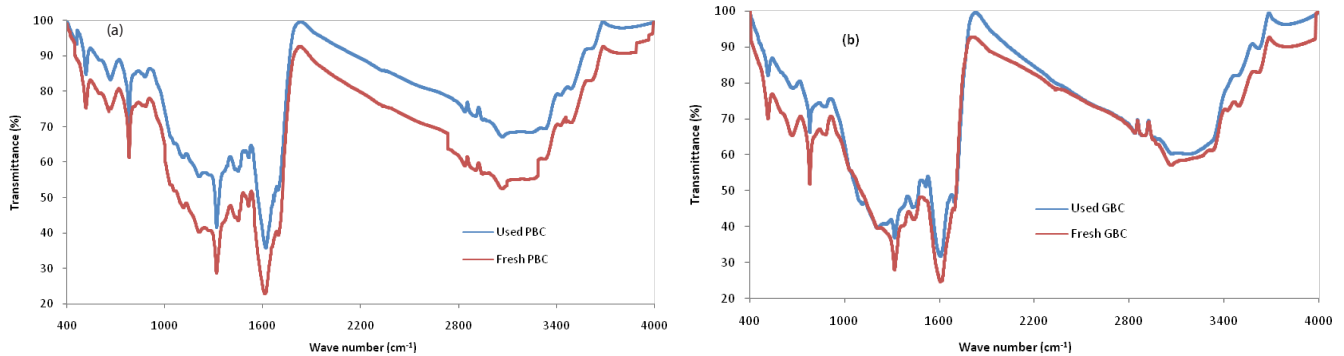


Fig. 11. FTIR spectra of: (a) PBC and (b) GBC.

Table 6

Groundwater and seawater treatment by PBC and GBC (adsorbent dose: 10 g/L, solution pH: as per original, contact time: 60 min, mixing intensity: 120 rpm)

Water quality	Sample 1: Groundwater			Sample 2: Seawater		
	Original concentration ^a	Concentration after treatment by		Original concentration ^a	Concentration after treatment by	
		PBC	GBC		PBC	GBC
F ⁻	3.1 + 10 ^b	1.82	2.36	0.75 + 10 ^b	2.34	3.18
NO ₃ ⁻	11	6	7	169	144	152
Cl ⁻	112.5	24	29	23,212	23,154	23,162
SO ₄ ²⁻	24	20	21	3,124	3,100	3,111
Total hardness	346	338	340	7,580	7,380	7,430
TDS	672	660	665	22,880	22,795	22,811
Hg ²⁺	0.005	–	–	0.02	–	–
Pb ²⁺	0.002	–	–	0.01	–	–
pH	7.2	7.1	7	8	7.8	7.9

^aThe unit for all parameters except total hardness (which is mg/L CaCO₃) is mg/L.

^bThe fluoride content of samples was spiked with 10 mg/L.

GBC and PBC under the optimized conditions to confirm their applicability. The initial pH of the samples was not adjusted to any particular value. After treating groundwater with GBC and PBC, the fluoride content was reduced by 81.9% and 86.1%, and at the same time, the pH increased to 7 and 7.1, respectively. Other contaminants such as Hg²⁺, Pb²⁺, and NO₃⁻ decreased significantly after treatment with GBC and PBC. For the more sophisticated medium, i.e., seawater, PBC was more efficient than GBC (Table 6). From the above decrease in fluoride concentration values, PBC has proven to be an excellent adsorbent for the removal of F⁻ ions from fluoride-laden waters.

4. Conclusions

In this study, powdered and granular adsorbents were prepared from *C. erectus* and tested for their potential in removing fluoride from aqueous solution and real water. The optimal conditions for fluoride adsorption by both adsorbents were identical at pH 6, adsorbent dose of 10 g/L, mixing intensity at 120 rpm, temperature of 20°C, and contact time for 60 min. The best-fitting adsorption isotherm and kinetic

models were the Langmuir and pseudo-second-order models for both types of adsorbents. PBC also afforded encouraging results with groundwater samples collected from endemic areas of Dashtestan, Iran, and Persian Gulf water. The maximum fluoride adsorption capacity of the PBC adsorbent is 205.70 mg/g according to the Langmuir isotherm, which is much higher than those of GBC (13.17 mg/g) and many other reported adsorbents. The results confirm that PBC is a more effective adsorbent than GBC for the removal of fluoride from aqueous solution.

Acknowledgment

The authors acknowledge the Bushehr University of Medical Sciences for providing necessary laboratory facilities during this study.

References

- [1] E.J. Reardon, Y. Wang, A limestone reactor for fluoride removal from wastewaters, *Environ. Sci. Technol.*, 34 (2000) 3247–3253.
- [2] F. Shen, X. Chen, P. Gao, G. Chen, Electrochemical removal of fluoride ions from industrial wastewater, *Chem. Eng. Sci.*, 58 (2003) 987–993.
- [3] D.T. Williams, G.L. LeBel, F.M. Benoit, Disinfection by-products in Canadian drinking water, *Chemosphere*, 34 (1997) 299–316.
- [4] X.-p. Liao, B. Shi, Adsorption of fluoride on zirconium(IV)-impregnated collagen fiber, *Environ. Sci. Technol.*, 39 (2005) 4628–4632.
- [5] S.V. Jadhav, E. Bringas, G.D. Yadav, V.K. Rathod, I. Ortiz, K.V. Marathe, Arsenic and fluoride contaminated groundwaters: a review of current technologies for contaminants removal, *J. Environ. Manage.*, 162 (2015) 306–325.
- [6] Y. Yu, C. Wang, X. Guo, J.P. Chen, Modification of carbon derived from *Sargassum* sp. by lanthanum for enhanced adsorption of fluoride, *J. Colloid Interface Sci.*, 441 (2015) 113–120.
- [7] J. Wang, W. Xu, L. Chen, Y. Jia, L. Wang, X.-J. Huang, J. Liu, Excellent fluoride removal performance by CeO₂-ZrO₂ nanocages in water environment, *Chem. Eng. J.*, 231 (2013) 198–205.
- [8] D. Mohan, A. Sarswat, Y.S. Ok, C.U. Pittman Jr., Organic and inorganic contaminants removal from water with biochar, a renewable, low cost and sustainable adsorbent – a critical review, *Bioresour. Technol.*, 160 (2014) 191–202.
- [9] X. Tan, Y. Liu, G. Zeng, X. Wang, X. Hu, Y. Gu, Z. Yang, Application of biochar for the removal of pollutants from aqueous solutions, *Chemosphere*, 125 (2015) 70–85.
- [10] X. Cao, L. Ma, B. Gao, W. Harris, Dairy-manure derived biochar effectively sorbs lead and atrazine, *Environ. Sci. Technol.*, 43 (2009) 3285–3291.
- [11] W. Zheng, M. Guo, T. Chow, D.N. Bennett, N. Rajagopalan, Sorption properties of greenwaste biochar for two triazine pesticides, *J. Hazard. Mater.*, 181 (2010) 121–126.
- [12] N. Karakoyun, S. Kubilay, N. Aktas, O. Turhan, M. Kasimoglu, S. Yilmaz, N. Sahiner, Hydrogel–Biochar composites for effective organic contaminant removal from aqueous media, *Desalination*, 280 (2011) 319–325.
- [13] M. Ahmad, S.S. Lee, X. Dou, D. Mohan, J.-K. Sung, J.E. Yang, Y.S. Ok, Effects of pyrolysis temperature on soybean stover- and peanut shell-derived biochar properties and TCE adsorption in water, *Bioresour. Technol.*, 118 (2012) 536–544.
- [14] H. Lu, W. Zhang, Y. Yang, X. Huang, S. Wang, R. Qiu, Relative distribution of Pb²⁺ sorption mechanisms by sludge-derived biochar, *Water Res.*, 46 (2012) 854–862.
- [15] A. Usman, A. Sallam, A. Al-Omran, A. El-Naggar, K. Alenazi, M. Nadeem, M. Al-Wabel, Chemically modified biochar produced from conocarpus wastes: an efficient sorbent for Fe(II) removal from acidic aqueous solutions, *Adsorpt. Sci. Technol.*, 31 (2013) 625–640.
- [16] M.I. Bautista-Toledo, J. Rivera-Utrilla, R. Ocampo-Pérez, F. Carrasco-Marín, M. Sanchez-Polo, Cooperative adsorption of bisphenol-A and chromium(III) ions from water on activated carbons prepared from olive-mill waste, *Carbon*, 73 (2014) 338–350.
- [17] G. Asgari, B. Ramavandi, S. Sahebi, Removal of a cationic dye from wastewater during purification by *Phoenix dactylifera*, *Desal. Wat. Treat.*, 52 (2014) 7354–7365.
- [18] M. Inyang, E. Dickenson, The potential role of biochar in the removal of organic and microbial contaminants from potable and reuse water: a review, *Chemosphere*, 134 (2015) 232–240.
- [19] D. Mohan, R. Sharma, V.K. Singh, P. Steele, C.U. Pittman Jr., Fluoride removal from water using bio-char, a green waste, low-cost adsorbent: equilibrium uptake and sorption dynamics modeling, *Ind. Eng. Chem. Res.*, 51 (2012) 900–914.
- [20] N.K. Mondal, R. Bhaumik, J.K. Datta, Removal of fluoride by aluminum impregnated coconut fiber from synthetic fluoride solution and natural water, *Alexandria Eng. J.*, 54 (2015) 1273–1284.
- [21] D. Mohan, S. Kumar, A. Srivastava, Fluoride removal from ground water using magnetic and nonmagnetic corn stover biochars, *Ecol. Eng.*, 73 (2014) 798–808.
- [22] A.K. Yadav, R. Abbassi, A. Gupta, M. Dadashzadeh, Removal of fluoride from aqueous solution and groundwater by wheat straw, sawdust and activated bagasse carbon of sugarcane, *Ecol. Eng.*, 52 (2013) 211–218.
- [23] A. Daifullah, S. Yakout, S. Elreefy, Adsorption of fluoride in aqueous solutions using KMnO₄-modified activated carbon derived from steam pyrolysis of rice straw, *J. Hazard. Mater.*, 147 (2007) 633–643.
- [24] B. Ramavandi, A. Rahbar, S. Sahebi, Effective removal of Hg²⁺ from aqueous solutions and seawater by *Malva sylvestris*, *Desal. Wat. Treat.*, 57 (2016) 23814–23826.
- [25] Z. Khademi, B. Ramavandi, M.T. Ghaneian, The behaviors and characteristics of a mesoporous activated carbon prepared from *Tamarix hispida* for Zn(II) adsorption from wastewater, *J. Environ. Chem. Eng.*, 3 (2015) 2057–2067.
- [26] Water Environment Federation, American Public Health Association, American Water Works Association, Standard Methods for the Examination of Water and Wastewater, Washington, D.C., USA, 2005.
- [27] G. Asgari, A.S. Mohammadi, S.B. Mortazavi, B. Ramavandi, Investigation on the pyrolysis of cow bone as a catalyst for ozone aqueous decomposition: kinetic approach, *J. Anal. Appl. Pyrolysis*, 99 (2013) 149–154.
- [28] B. Ramavandi, Treatment of water turbidity and bacteria by using a coagulant extracted from *Plantago ovata*, *Water Resour. Ind.*, 6 (2014) 36–50.
- [29] G. Asgari, B. Roshani, G. Ghanizadeh, The investigation of kinetic and isotherm of fluoride adsorption onto functionalize pumice stone, *J. Hazard. Mater.*, 217 (2012) 123–132.
- [30] G. Karthikeyan, S.S. Ilango, Fluoride sorption using Moringa Indica-based activated carbon, *J. Environ. Health Sci. Eng.*, 4 (2007) 21–28.
- [31] K.D. Brahman, T.G. Kazi, J.A. Baig, H.I. Afridi, S.S. Arain, S. Saraj, M.B. Arain, S.A. Arain, Biosorptive removal of inorganic arsenic species and fluoride from aqueous medium by the stem of *Tecomella undulate*, *Chemosphere*, 150 (2016) 320–328.
- [32] R. Mariappan, R. Vairamuthu, A. Ganapathy, Use of chemically activated cotton nut shell carbon for the removal of fluoride contaminated drinking water: kinetics evaluation, *Chin. J. Chem. Eng.*, 23 (2015) 710–721.
- [33] A. Moubarik, N. Grimi, Valorization of olive stone and sugar cane bagasse by-products as biosorbents for the removal of cadmium from aqueous solution, *Food Res. Int.*, 73 (2015) 169–175.
- [34] A. Bhatnagar, E. Kumar, M. Sillanpää, Fluoride removal from water by adsorption—a review, *Chem. Eng. J.*, 171 (2011) 811–840.
- [35] M.A.T. Ajisha, K. Rajagopal, Fluoride removal study using pyrolyzed *Delonix regia* pod, an unconventional adsorbent, *Int. J. Environ. Sci. Technol.*, 12 (2015) 223–236.

- [36] S. Dawood, T.K. Sen, Removal of anionic dye Congo red from aqueous solution by raw pine and acid-treated pine cone powder as adsorbent: equilibrium, thermodynamic, kinetics, mechanism and process design, *Water Res.*, 46 (2012) 1933–1946.
- [37] G. Asgari, B. Roshani, G. Ghanizadeh, The investigation of kinetic and isotherm of fluoride adsorption onto functionalize pumice stone, *J. Hazard. Mater.*, 217–218 (2012) 123–132.
- [38] A.B. Nasr, K. Walha, C. Charcosset, R.B. Amar, Removal of fluoride ions using cuttlefish bones, *J. Fluorine Chem.*, 132 (2011) 57–62.
- [39] R. Khosravi, M. Fazlzadehdavil, B. Barikbin, A.A. Taghizadeh, Removal of hexavalent chromium from aqueous solution by granular and powdered *Peganum Harmala*, *Appl. Surf. Sci.*, 292 (2014) 670–677.
- [40] S. Wu, K. Zhang, J. He, X. Cai, K. Chen, Y. Li, B. Sun, L. Kong, J. Liu, High efficient removal of fluoride from aqueous solution by a novel hydroxyl aluminum oxalate adsorbent, *J. Colloid Interface Sci.*, 464 (2016) 238–245.
- [41] Z.Z. Ismail, H.N. AbdelKareem, Sustainable approach for recycling waste lamb and chicken bones for fluoride removal from water followed by reusing fluoride-bearing waste in concrete, *Waste Manage.*, 45 (2015) 66–75.
- [42] A. Rezaee, B. Ramavandi, F. Ganati, M. Ansari, A. Solimani, Biosorption of mercury by biomass of filamentous algae *Spirogyra* species, *J. Biol. Sci.*, 6 (2006) 695–700.
- [43] M. Sujana, R. Thakur, S. Rao, Removal of fluoride from aqueous solution by using alum sludge, *J. Colloid Interface Sci.*, 206 (1998) 94–101.
- [44] B.-S. Zhu, Y. Jia, Z. Jin, B. Sun, T. Luo, X.-Y. Yu, L.-T. Kong, X.-J. Huang, J.-H. Liu, Controlled synthesis of natroalunite microtubes and spheres with excellent fluoride removal performance, *Chem. Eng. J.*, 271 (2015) 240–251.
- [45] S.B. Ghosh, R. Bhaumik, N.K. Mondal, Optimization study of adsorption parameters for removal of fluoride using aluminium-impregnated potato plant ash by response surface methodology, *Clean Technol. Environ. Policy*, 18 (2016) 1069–1083.
- [46] S. Dong, Y. Wang, Characterization and adsorption properties of a lanthanum-loaded magnetic cationic hydrogel composite for fluoride removal, *Water Res.*, 88 (2016) 852–860.
- [47] G. Asgari, B. Ramavandi, S. Farjadfard, Abatement of azo dye from wastewater using bimetal-chitosan, *Scientific World J.*, 2013 (2013) 1–10.
- [48] R. Sun, H.-B. Zhang, J. Qu, H. Yao, J. Yao, Z.-Z. Yu, Supercritical carbon dioxide fluid assisted synthesis of hierarchical AlOOH@ reduced graphene oxide hybrids for efficient removal of fluoride ions, *Chem. Eng. J.*, 292 (2016) 174–182.
- [49] M. Ahmadi, E. Kouhgardi, B. Ramavandi, Physico-chemical study of dew melon peel biochar for chromium attenuation from simulated and actual wastewaters, *Korean J. Chem. Eng.*, 33 (2016) 2589–2601.
- [50] M. Fooladvand, B. Ramavandi, Adsorption potential of NH₄Br-soaked activated carbon for cyanide removal from wastewater, *Indian J. Chem. Technol.*, 22 (2015) 183–193.
- [51] V.K. Gupta, I. Ali, V.K. Saini, Defluoridation of wastewaters using waste carbon slurry, *Water Res.*, 41 (2007) 3307–3316.
- [52] M. Brigante, M. Avena, Biotemplated synthesis of mesoporous silica for doxycycline removal. Effect of pH, temperature, ionic strength and Ca²⁺ concentration on the adsorption behaviour, *Microporous Mesoporous Mater.*, 225 (2016) 534–542.
- [53] I. Ali, Z.A. Allothman, M.M. Sanagi, Green synthesis of iron nano-impregnated adsorbent for fast removal of fluoride from water, *J. Mol. Liq.*, 211 (2015) 457–465.
- [54] R.K. Bharali, K.G. Bhattacharyya, Biosorption of fluoride on Neem (*Azadirachta indica*) leaf powder, *J. Environ. Chem. Eng.*, 3 (2015) 662–669.